DNA methylation profiles in precancerous tissue and cancers: carcinogenetic risk estimation and prognostication based on DNA methylation status

Alterations in DNA methylation, which are associated with DNA methyltransferase abnormalities and result in silencing of tumor-related genes and chromosomal instability, are involved even in precancerous changes in various organs. DNA methylation alterations also account for the histological heterogeneity and clinicopathological diversity of human cancers. Therefore, we have analyzed DNA methylation on a genome-wide scale in clinical tissue samples. Our approach using the bacterial artificial chromosome array-based methylated CpG island amplification method has revealed that DNA methylation alterations correlated with the future development of more malignant cancers are already accumulated at the precancerous stage in the kidney, liver and urinary tract. DNA methylation profiles at precancerous stages are basically inherited by the corresponding cancers developing in individual patients. Such DNA methylation alterations may confer vulnerability to further genetic and epigenetic alterations, generate more malignant cancers, and thus determine patient outcome. On the basis of bacterial artificial chromosome array-based methylated CpG island amplification data, indicators for carcinogenetic risk estimation have been established using liver tissue specimens from patients with hepatitis virus infection, chronic hepatitis and liver cirrhosis or histologically normal urothelia, and for prognostication using biopsy or surgically resected specimens from patients with renal cell carcinoma, hepatocellular carcinoma and urothelial carcinoma. Such genome-wide DNA methylation profiling has now firmly established the clinical relevance of translational epigenetics.

KEYWORDS: bacterial artificial chromosome array-based methylated CpG island amplification ■ DNA methylation ■ DNA methyltransferase ■ precancerous condition ■ prognostication ■ risk estimation

Eri Arai[1] & Yae Kanai[†1]

[1]Pathology Division, National Cancer Center Research Institute, 5-1-1 Tsukiji, Chuo-ku, Tokyo 104-0045, Japan
[†]Author for correspondence:
Tel.: +81 335 422 511
Fax: +81 332 482 463
ykanai@ncc.go.jp

DNA methylation, a covalent chemical modification resulting in the addition of a methyl group at the carbon 5 position of the cytosine ring in CpG dinucleotides, is one of the most consistent epigenetic changes occurring in human cancers [1–3]. DNA methylation normally promotes a highly condensed heterochromatin structure associated with deacetylation of histones H3 and H4, loss of histone H3 lysine 4 (H3K4) methylation, and gain of H3K9 and H3K27 methylation [4–6]. DNA methylation is a stable modification inherited throughout successive cell divisions, and is essential for X-chromosome inactivation, genome imprinting, silencing of transposons and other parasitic elements, and proper expression of genes [7].

Human cancer cells show a drastic change in DNA methylation status, specificity in the overall DNA hypomethylation and regional DNA hypermethylation [1–3]. In 1995, when the *RB* and *VHL* genes were the only tumor suppressor genes known to be silenced by DNA methylation, we showed for the first time that the E-cadherin tumor suppressor gene is silenced by DNA methylation around the promoter region [8], and proposed the universality of a 'two-hit' mechanism involving DNA hypermethylation and loss of heterozygosity during carcinogenesis. The list of tumor-related genes whose levels of expression are altered owing to DNA hypo- or hypermethylation has been increasing [9]. At this point, some explanation is necessary regarding the mechanisms whereby tumor-related genes whose DNA methylation status is altered during carcinogenesis are selected. One, but likely not the only, explanation for such selection is polycomb binding, in which CpG-rich sequences targeted by the polycomb complex in normal embryonic stem cells consequently form a bivalent domain carrying both 'activating' H3K4 methylation and 'inactivating' H3K27 methylation [10]. This bivalent state is converted to a primary active or repressive chromatin conformation after differentiation cues have been received. During carcinogenesis, such modifications may render the genes vulnerable to errors, resulting in aberrant DNA methylation [11].

On the other hand, DNA hypomethylation induces chromosomal instability through decondensation of heterochromatin and enhancement

10.2217/EPI.10.16 © 2010 Future Medicine Ltd

ISSN 1750-1911

of chromosomal recombination during carcinogenesis [12]. For example, in hepatocellular carcinoma (HCC) [13] and urothelial carcinoma (UC) [14], DNA hypomethylation of pericentromeric satellite regions is correlated with copy number alterations on chromosomes 1 and 9, where such regions are found abundantly. A DNA methyltransferase (DNMT), DNMT3b, is required for DNA methylation of pericentromeric satellite regions in early mouse embryos [15]. We have demonstrated the possibility that an inactive splice variant, DNMT3b4 is upregulated, competes with DNMT3b3, the major splice variant in normal liver tissue, for targeting to pericentromeric satellite regions, and may lead to chromosomal instability through induction of DNA hypomethylation in such regions during hepatocarcinogenesis [16].

Translational epigenetics has now come of age [17–19], and the empirical analysis of DNA methylation status in clinical tissue samples with reference to the clinicopathological parameters of human cancers is becoming increasingly important for the diagnosis, prevention and therapy of cancers [20–22].

DNA methylation alterations during multistage carcinogenesis

Accumulating evidence suggests that alterations of DNA methylation may play a significant role even at precancerous stages in association with chronic inflammation, persistent infection with viruses and other pathogenic microorganisms, such as hepatitis B virus (HBV) or hepatitis C virus (HCV) [23–25], Epstein–Barr virus [26], human papillomavirus [27], and *Helicobacter pylori* [28] and cigarette smoking [29]. In the 1990s, we frequently observed DNA hypermethylation on C-type CpG islands, which are generally methylated in a cancer-specific but not age-dependent manner [30], and DNA methylation alterations at 'hot spots' of loss of heterozygosity in HCCs, even in samples of noncancerous liver tissue showing chronic hepatitis or liver cirrhosis, which are widely considered to be precancerous conditions, in comparison with normal liver tissue samples [23–25]. These findings [23] represented some of the earliest reports of DNA methylation alterations at the precancerous stage. Silencing of the E-cadherin gene, which encodes a Ca^{2+}-dependent cell–cell adhesion molecule, in samples of noncancerous liver tissue showing chronic hepatitis or cirrhosis may result in heterogeneous E-cadherin expression, which is associated with small focal areas where hepatocytes show only slight E-cadherin immunoreactivity [31]. Silencing of the E-cadherin gene may participate even in the very early stage of hepatocarcinogenesis through loss of intercellular adhesiveness and destruction of tissue morphology. Expression levels of mRNA for DNMT1, the major and best known DNMT, are significantly higher in 48 samples of noncancerous liver tissue showing chronic hepatitis or cirrhosis than in normal liver tissue, and are even higher in 67 samples of HCCs [32]. The incidence of DNMT1 overexpression in 53 samples of HCCs is significantly correlated with poorer tumor differentiation and portal vein involvement [33]. Moreover, the recurrence-free and overall survival rates of patients with HCCs showing DNMT1 overexpression are significantly lower than those of patients with HCCs that do not [33].

Ductal carcinomas of the pancreas frequently develop after chronic damage owing to pancreatitis. At least a proportion of peripheral pancreatic ductal epithelia with an inflammatory background may be at precancerous stages. We conducted an immunohistochemical analysis of DNMT1 in 48 samples of peripheral pancreatic duct epithelia showing no remarkable histological findings without an inflammatory background, 54 samples of peripheral pancreatic duct epithelia with an inflammatory background, 188 samples of another precancerous lesion, pancreatic intraepithelial neoplasia (PanIN), and 220 areas of invasive ductal carcinoma from surgical specimens resected from 100 patients (5, 24, 49 and 22 patients at Stage I to II, III, IVa and IVb, respectively) [34]. DNA methylation status of the *p14, p15, p16, p73, APC, hMLH1, MGMT, BRCA1, GSTP1, TIMP-3, CDH1* and *DAPK-1* genes was also analyzed in tissue samples during pancreatic carcinogenesis. To examine DNA methylation status in tiny tissue samples of peripheral pancreatic duct epithelia without or with an inflammatory background, avoiding any contamination with surrounding acinar cells and/or lymphocytes, we employed a method combining tissue microdissection with agarose bead-based bisulfite conversion followed by nested methylation-specific PCR: preheated low-melting agarose was mixed with the harvested microdissected tissue samples and the mixtures were pipetted into chilled mineral oil to form agarose beads. The beads with the tissue were incubated with proteinase K followed by bisulfite conversion. After neutralization with hydrochloric acid, the beads were used directly for nested methylation-specific PCR. This method also allowed us to examine the DNA methylation

status in PanIN and ductal carcinoma, avoiding contamination by the abundant desmoplastic stroma. The incidence of DNMT1 protein expression [34] and the average number of methylated tumor-related genes [35] increased with progression from peripheral pancreatic ductal epithelia with an inflammatory background, to PanIN, to well differentiated ductal carcinoma, and finally, to a poorly differentiated ductal carcinoma, in comparison with normal peripheral pancreatic duct epithelia without an inflammatory background. DNMT1 overexpression in ductal carcinomas of the pancreas is significantly correlated with the extent of invasion to the surrounding tissue, an advanced stage, poorer patient outcome [34], and accumulation of DNA methylation of tumor-related genes [35]. Although the maintenance activities of DNMT1 are related to its *in vitro* preference for hemimethylated substrates [36], excessive amounts of DNMT1 in comparison to those of proliferating cell nuclear antigen, which targets DNMT1 to replication foci [37], may participate in *de novo* methylation of CpG islands [38]. In fact, significant correlation between DNMT1 overexpression and accumulation of DNA methylation of specific genes in cell lines, mouse models and clinical tissue samples of various cancers has also been reported by other groups [39–43]. However, other groups have stated that they did not find such significant correlations [44–46]. Therefore, the participation of DNMT1 overexpression in accumulation of DNA methylation of tumor-related genes remains a controversial issue.

Genome-wide DNA methylation analysis

Recently, it has become possible to analyze DNA methylation on a genome-wide scale. The fact that DNA methylation alterations are associated with multistage carcinogenesis has prompted us to perform such genome-wide analysis in tissue specimens. The methods most commonly used to read methylated cytosines are a DNA methylation-sensitive restriction enzyme-based approach, such as the well-established technique of methylated CpG island amplification [47], affinity-based approaches, whereby antimethylcytosine antibody or methyl-binding domain proteins are used to enrich methylated fractions of genomic DNA, and bisulfite conversion of non-methylated cytosines to thymidine through hydrolytic deamination. These strategies for revealing methylated cytosines have been applied mainly to array platforms [48], and the resolution of the microarrays has been markedly improved [49,50]. In addition to the introduction of new-generation sequencing technologies for bisulfite-converted genomic sequencing [48], a high-throughput technique without bisulfite conversion has been developed based on single-molecule, real-time DNA sequencing [51]. These new technologies will be able to efficiently reveal genome-wide DNA methylation profiles in tissue samples.

At the present time, many researchers in the field of cancer epigenetics use mainly promoter arrays to identify the genes that are silenced by DNA methylation in cancer cells. However, the promoter regions of specific genes are not the only target of DNA methylation alterations in human cancers. DNA methylation status in genomic regions that do not directly participate in gene silencing, such as the edges of CpG islands, may be altered at precancerous stages before the alterations of the promoter regions themselves occur [52]. Genomic regions in which DNA hypomethylation affects chromosomal instability may not be contained in promoter arrays. Moreover, aberrant DNA methylation of large regions of chromosomes, which are regulated in a coordinated manner in human cancers owing to a process of long-range epigenetic silencing, has recently attracted attention [53]. Therefore, we have recently employed bacterial artificial chromosome (BAC) array-based methylated CpG island amplification (BAMCA; Figure 1) [54]. Test or reference DNA was first digested with the methylation-sensitive restriction enzyme *Sma*I and subsequently with the methylation-insensitive *Xma*I. Adapters were ligated to the *Xma*I-digested sticky ends, and PCR was performed with an adapter primer set. Test and reference PCR products were labeled by random priming with Cy3- and Cy5-dCTP, respectively, and precipitated together with ethanol in the presence of Cot-I DNA. The mixture was applied to a custom-made array harboring approximately 4500 BAC clones located throughout chromosomes 1 to 22, X and Y.

Even though the resolution of BAMCA is inferior to the abovementioned newly developed high-resolution arrays, BAMCA has an ability for detecting any tendency for coordinated regulation of DNA methylation at multiple CpG sites in individual large regions of chromosomes, because any region covered by one BAC contains multiple *Sma*I sites. In fact, we validated this ability by the quantitative evaluation of DNA methylation status at each *Sma*I site on representative BAC clones by pyrosequencing: when almost all *Sma*I sites on

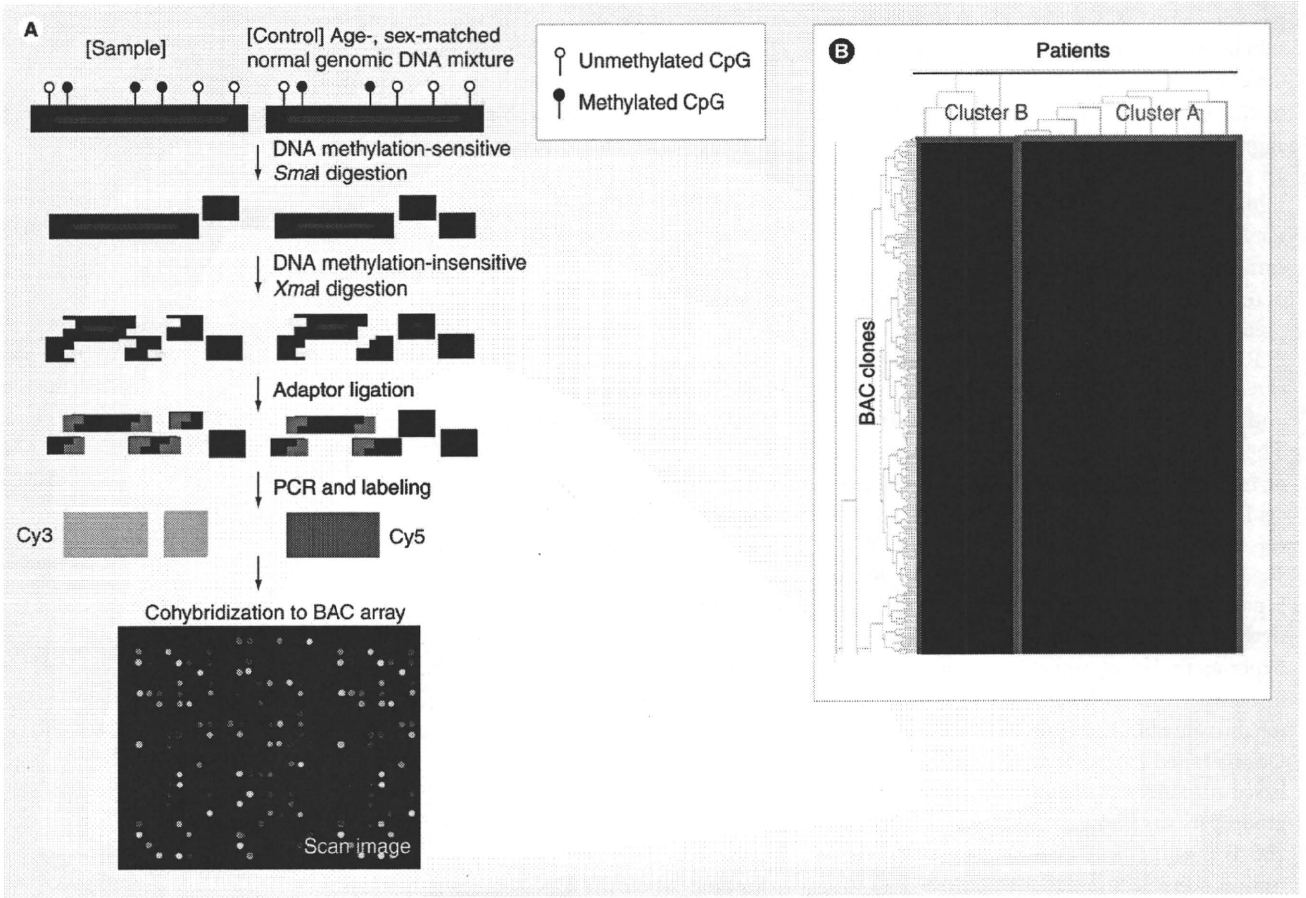

Figure 1. Bacterial artificial chromosome array-based methylated CpG island amplification in tissue samples.
(A) BAC array-based methylated CpG island amplification (BAMCA) method and an example of a scan image. **(B)** An example of unsupervised 2D hierarchical clustering analysis of patients with cancers based on BAMCA data. Patients with cancers are frequently clustered into subclasses associated with distinct DNA methylation profiles and distinct clinicopathological parameters.
BAC: Bacterial artificial chromosome.

a BAC clone simultaneously showed lower or higher DNA methylation rates in comparison with those of normal tissues by pyrosequencing, the signal ratio on the BAC clone demonstrated by BAMCA showed DNA hypo- or hyper-methylation, respectively [55]. BAMCA has also been used by other groups to identify tumor-related genes whose expression levels are regulated by DNA methylation in human cancer cells [56–58].

Genome-wide DNA methylation profiles in precancerous stages are inherited by cancers & determine the tumor aggressiveness

With respect to renal cell carcinomas (RCCs), DNA methylation profiling of more than 800 genes has been reported in both Von Hippel Lindau-related and -unrelated RCCs, and it is known that genes linked to TGF-β or ERK/Akt signaling are preferentially methylated in papillary RCCs in comparison to clear cell RCCs [59]. However, precancerous conditions in the kidney have rarely been described because of the lack of any remarkable histological changes, or association with chronic inflammation and persistent infection with viruses or other pathogenic microorganisms. The DNA methylation status of noncancerous renal tissues obtained from patients with RCCs has not been analyzed in detail. When BAMCA methods were applied to 51 samples of noncancerous renal tissue obtained from patients with clear cell RCCs, many BAC clones showed DNA hypo- or hyper-methylation in comparison to normal renal tissue samples from patients without any primary renal tumors [60]. From the viewpoint of DNA methylation, we can consider that noncancerous renal tissue from patients with RCCs is already at precancerous stages, showing genome-wide DNA methylation alterations [60].

We then performed unsupervised 2D hierarchical clustering analysis based on BAMCA data for noncancerous renal tissue samples. The

patients with RCCs were clustered into two subclasses, clusters A_{NK} and B_{NK} [60]. Tumors developing in individual patients belonging to cluster B_{NK} were clinicopathologically more aggressive than those in cluster A_{NK}. The overall survival rate of patients in cluster B_{NK} was significantly lower than that of patients in cluster A_{NK}. Aggressiveness of the corresponding tumors and even patient outcome may thus be determined by DNA methylation profiles at precancerous stages.

Renal cell carcinomas are usually well demarcated, being surrounded by a fibrous capsule, and hardly ever contain a fibrous stroma. Therefore, we were able to obtain cancer cells of high purity from fresh surgical specimens, avoiding contamintation with both noncancerous epithelial cells and stromal cells. When we analyzed 51 samples of RCC (30, 16 and 5 patients at Stage I to II, III and IV, respectively), more BAC clones showed DNA hypo- or hyper-methylation, and its degree was increased in comparison with samples of noncancerous renal tissue obtained from patients with RCCs. Unsupervised 2D hierarchical clustering analysis based on BAMCA data for RCCs was able to group patients into two subclasses, clusters A_{TK} and B_{TK} [60]. Clinicopathologically aggressive tumors were accumulated in cluster B_{TK}. The overall survival rate of patients in cluster B_{TK} was significantly lower than that of patients in cluster A_{TK}.

All patients who were grouped in cluster B_{NK} on the basis of BAMCA data for noncancerous renal tissue were included in cluster B_{TK} on the basis of BAMCA data for the RCCs themselves [60]. The majority of the BAC clones significantly discriminating cluster B_{NK} from cluster A_{NK} also discriminated cluster B_{TK} from cluster A_{TK}. Among BAC clones characterizing both clusters B_{NK} and B_{TK}, where the average signal ratio of cluster B_{NK} was higher than that of cluster A_{NK}, the average signal ratio of cluster B_{TK} was also higher than that of cluster A_{TK} without exception (FIGURE 2A). Among BAC clones characterizing both clusters B_{NK} and B_{TK}, where the average signal ratio of cluster B_{NK} was lower than that of cluster A_{NK}, the average signal ratio of cluster B_{TK} was also lower than that of cluster A_{TK} without exception (FIGURE 2A). Comparison between the signal ratios of each BAC clone characterizing both clusters B_{NK} and B_{TK} revealed that the DNA methylation status of the noncancerous renal tissue was basically inherited by the corresponding RCC in each individual patient (FIGURE 2B) [60].

In noncancerous renal tissue showing no remarkable histological changes and consisting mainly of renal tubules with specialized functions, no progenitor cell is able to gain a growth advantage, and clonal expansion is unable to occur. Therefore, the distinct DNA methylation profiles of cluster B_{NK} cannot be established through the selection of one of a number of random DNA methylation profiles in noncancerous renal tissue, and instead may be established through distinct target mechanisms. Since the DNA methylation profiles in cluster B_{TK} are shared by phenotypically similar patients, who all suffer from clinicopathologically aggressive tumors and show a poor outcome, DNA methylation alterations in at least a proportion of the BAC regions characterizing cluster B_{TK} cannot be passenger changes. DNA methylation alterations of BAC regions characterizing cluster B_{TK} may significantly participate in carcinogenesis, since the DNA methylation profiles in cluster B_{NK} were established at very early stages of carcinogenesis and inherited during progression of the cancers themselves as cluster B_{TK}. At least a proportion of DNA methylation alterations at precancerous stages may be 'epigenetic gatekeepers' [2], which allow time for further epigenetic and genetic alterations.

In fact, when the DNA methylation status on CpG islands of the *p16*, *hMLH1*, *VHL* and *THBS-1* genes, and the methylated in tumor (MINT)-1, -2, -12, -25 and -31 clones were examined by bisulfite modification in the same cohort, genome-wide DNA methylation alterations consisting of both hypo- and hypermethylation revealed by BAMCA in cluster B_{TK} were frequently associated with accumulation of regional DNA hypermethylation on these CpG islands [61]. For comparison with BAMCA data, we also examined copy number alterations by array-based comparative genomic hybridization using the same BAC array in the same cohort. By unsupervised hierarchical clustering analysis based on copy number alterations, RCCs were clustered into the two subclasses, clusters GA_{TK} and GB_{TK} [62]. Copy number alterations were accumulated in the cluster GB_{TK}. Loss of chromosome 3p and gain of 5q and 7 were frequent in both clusters GA_{TK} and GB_{TK}, whereas loss of 1p, 4, 9, 13q and 14q was frequent only in cluster GB_{TK} [62]. Clear cell RCCs showing higher histological grades, vascular involvement, renal vein tumor thrombi and higher pathological stages were accumulated in cluster GB_{TK} [62]. The recurrence-free and overall survival rates of patients in cluster GB_{TK} were

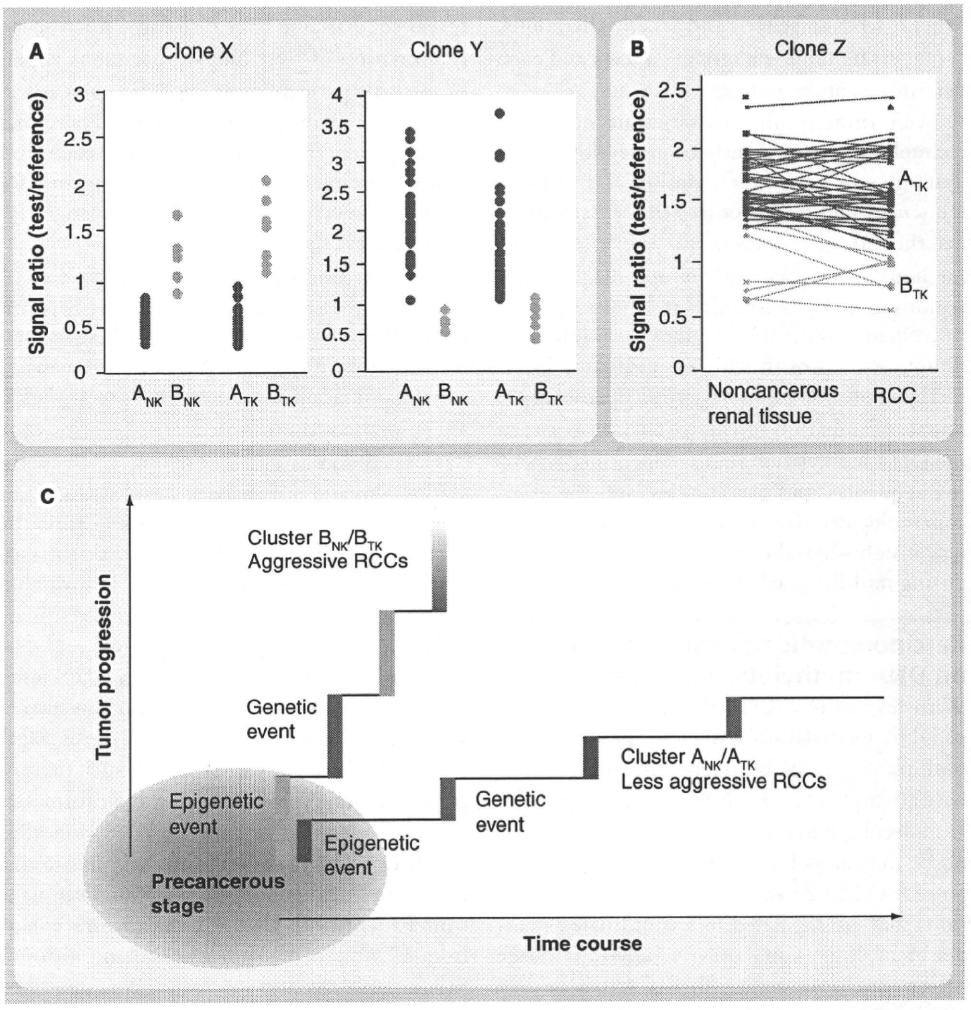

Figure 2. DNA methylation profiles in precancerous conditions and renal cell carcinomas.
(A) Correlation between DNA methylation profiles of precancerous conditions and those of RCCs. Cluster B_{NK} was completely included in cluster B_{TK}. The majority of the bacterial artificial chromosome (BAC) clones, 724 in all, significantly discriminating cluster B_{NK} from cluster A_{NK}, also discriminated cluster B_{TK} from cluster A_{TK}. In 311 of the 724 BAC clones, where the average signal ratio of cluster B_{NK} was higher than that of cluster A_{NK}, such as clone X, the average signal ratio of cluster B_{TK} was also higher than that of cluster A_{TK} without exception. In 413 of the 724 BAC clones, where the average signal ratio of cluster B_{NK} was lower than that of cluster A_{NK}, such as clone Y, the average signal ratio of cluster B_{TK} was also lower than that of cluster A_{TK} without exception. **(B)** Scattergram of the signal ratios in samples of noncancerous renal tissue and RCCs for all patients examined for a representative BAC clone, clone Z. The DNA methylation status of the noncancerous renal tissue was basically inherited by the corresponding RCC in individual patients. **(C)** Significance of DNA methylation alterations at precancerous stages. Regional DNA hypermethylation of C-type CpG islands and copy number alterations were accumulated in cluster B_{TK}. In other words, DNA methylation alterations in precancerous conditions, such as DNA methylation profiles corresponding to cluster B_{NK}, may not occur randomly but may be prone to further accumulation of epigenetic and genetic alterations, thus generating more malignant cancers, such as the RCCs in patients belonging to cluster B_{TK}.
RCC: Renal cell carcinoma.

significantly lower than those of patients in cluster GA_{TK} [62]. Multivariate analysis revealed that genetic clustering was a predictor of recurrence-free survival, and was independent of histological grade and pathological stage [62]. A subclass of cluster B_{TK} based on BAMCA data was completely included in cluster GB_{TK} showing accumulation of copy number alterations. Genetic and epigenetic alterations are not mutually exclusive during renal carcinogenesis, and particular DNA methylation profiles may be closely related to chromosomal instability. DNA methylation alterations at precancerous stages, which may not occur randomly but may

foster further epigenetic and genetic alterations, can generate more malignant cancers and even determine patient outcome (FIGURE 2C).

Even though high-throughput detection technologies have recently been developed, the dynamics of DNA methylation at repetitive sequences and gene bodies still remain to be determined [7]. However, our BAC array-based methods do not focus only on specific promoter regions and CpG islands, and have successfully identified the BAC regions including non-unique sequences in which coordinated DNA methylation alterations have clinicopathological impact. Evaluation of the correlation between the DNA methylation status of identified repetitive sequences and gene bodies, and the clinicopathological diversity of cancers may provide new insights into the roles of DNA methylation during multistage carcinogenesis.

Carcinogenetic risk estimation based on DNA methylation profiles

With respect to HCCs, the results of analysis of DNA methylation status of CpG islands of multiple genes have been reported. Some groups have attempted to use DNA methylation profiles as molecular markers of early HCCs or as prognostic indicators for patients with HCCs [63,64]. Since BAMCA detects DNA methylation alterations that are regulated in a coordinated manner at multiple CpG sites in individual large regions of chromosomes, BAMCA may be able to identify unique diagnostic indicators that may be overlooked by other technologies. We then applied the BAMCA method to multistage hepatocarcinogenesis. HCCs are known to be medullary tumors without a fibrous stroma. Therefore, we were able to obtain cancer cells of high purity from fresh surgical specimens, avoiding any contamination with stromal cells. In samples of noncancerous liver tissue obtained from patients with HCCs, many BAC clones showed DNA hypo- or hyper-methylation in comparison with normal liver tissue from patients without HCCs. Patients showing DNA hypo- or hyper-methylation on more BAC clones in their samples of noncancerous liver tissue frequently developed metachronous or recurrent HCCs after hepatectomy [65], suggesting that DNA methylation alterations at precancerous stages may not occur randomly but tend to lead to the development of more malignant HCCs.

The effectiveness of surgical resection for HCC is limited, unless the disease is diagnosed early at the asymptomatic stage. Therefore, surveillance at precancerous stages is a priority. To reveal the baseline liver histology, microscopy examination of liver biopsy specimens is performed for patients with hepatitis virus infection prior to interferon therapy. Therefore, carcinogenetic risk estimation using such liver biopsy specimens would be advantageous for close follow-up of patients who are at high risk of HCC development.

Inflammation itself can induce drastic DNA methylation alterations at the chronic hepatitis stage. Although a proportion of such alterations do participate in progression to HCC, the remaining inflammation-associated DNA methylation alterations may diminish after the hepatitis stage has passed and as HCC develops. DNA methylation alterations associated only with inflammation and not with carcinogenesis cannot be regarded as indicators for carcinogenetic risk estimation in patients who are being followed up owing to chronic hepatitis. Therefore, to estimate the degree of carcinogenetic risk based on DNA methylation profiles, we focused on BAC clones for which DNA methylation status was altered at the chronic hepatitis and liver cirrhosis stages and were inherited by HCCs from such precancerous stages. Among them, a bioinformatics approach identified the top 25 BAC clones for which DNA methylation status was able to discriminate 15 samples of noncancerous liver tissue from patients with HCCs in the learning cohort from 10 samples of normal liver tissue with sufficient sensitivity and specificity. We established the criteria for carcinogenetic risk estimation by combining the cutoff values of signal ratios for the 25 BAC clones (FIGURE 3A). Based on these criteria, the sensitivity and specificity for diagnosis of noncancerous liver tissue samples obtained from patients with HCCs in the learning cohort as being at high risk of carcinogenesis were both 100% [65]. Our criteria enabled diagnosis of additional noncancerous liver tissue samples obtained from patients with HCCs in the validation cohort (n = 50) as being at high risk of carcinogenesis with a sensitivity and specificity of 96% [65].

The number of BAC clones satisfying the criteria in noncancerous liver tissue samples showing chronic hepatitis obtained from patients with HCCs was not significantly different from that in noncancerous liver tissue samples showing cirrhosis obtained from patients with HCCs. In addition, the average number of BAC clones satisfying the criteria was significantly lower in samples of liver tissue obtained from patients who were infected with HBV or HCV, but who had never developed HCCs, than that in noncancerous liver tissue samples obtained from

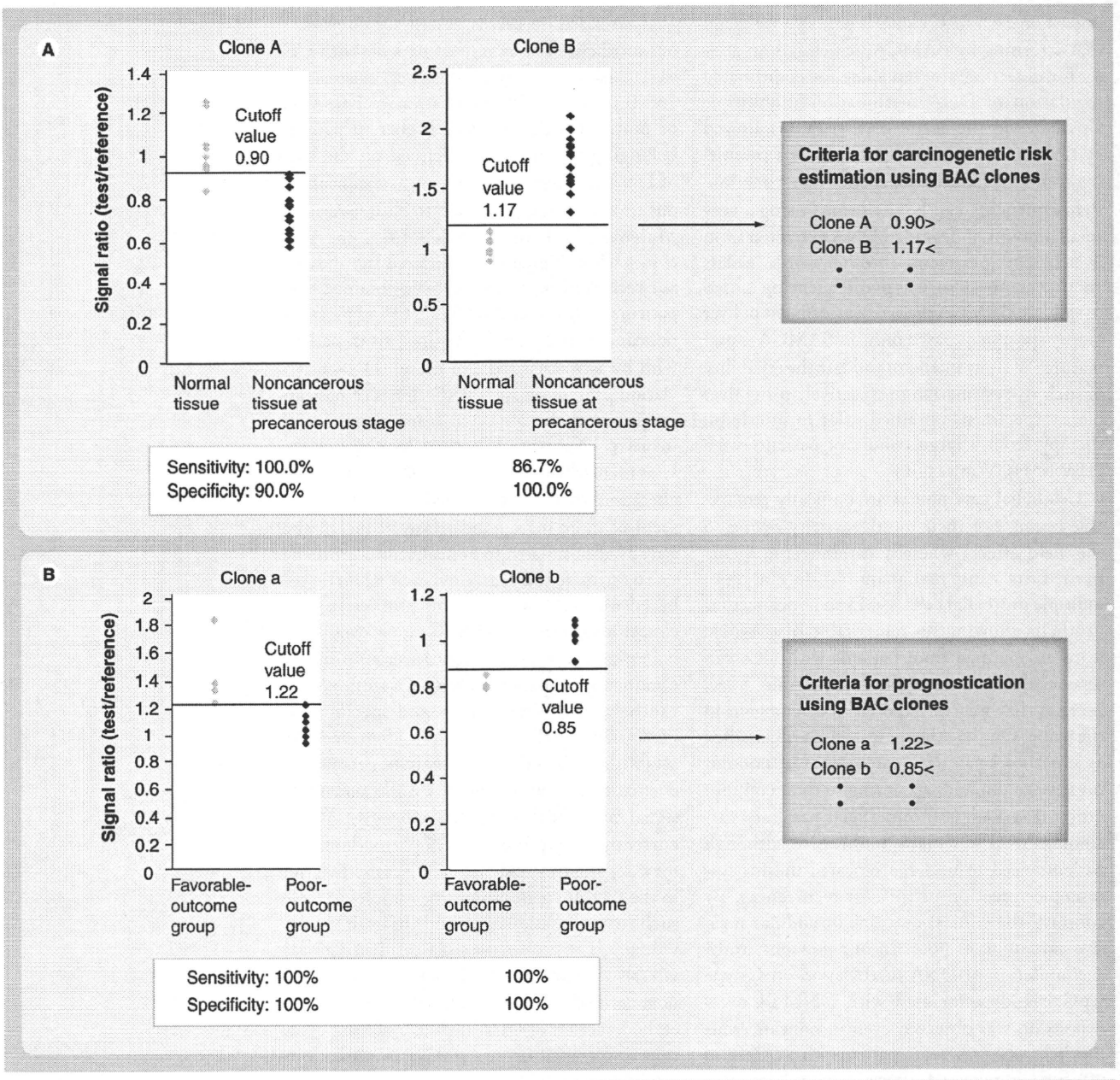

Figure 3. Carcinogenetic risk estimation and prognostication of patients with cancers based on DNA methylation status.
(A) Carcinogenetic risk estimation based on DNA methylation status. Examples of scattergrams of the signal ratios in normal tissue samples and noncancerous tissue samples at precancerous stages for representative BAC clones, clone A and clone B. Using the cutoff values in each panel, noncancerous tissue samples at precancerous stages were discriminated from normal tissue samples with sufficient sensitivity and specificity. Based on a combination of the cutoff values for the selected BAC clones, the criteria for carcinogenetic risk estimation were established. **(B)** Prognostication of patients with cancers based on DNA methylation status. Examples of scattergrams of the signal ratios in the favorable-outcome group and poor-outcome group for representative BAC clones, clone a and clone b. Using the cutoff values in each panel, patients belonging to the poor-outcome group were discriminated from those belonging to the favorable-outcome group. Based on a combination of the cutoff values for the selected BAC clones, the criteria for prognostication were established.
BAC: Bacterial artificial chromosome.

patients with HCCs. Therefore, our criteria may be applicable for classifying liver tissue obtained from patients who are followed up because of hepatitis virus infection, chronic hepatitis or liver cirrhosis into that which may generate HCCs and that which will not [65].

Next, we quantitatively examined the DNA methylation status at each *Xma*I/*Sma*I site on the 25 BAC clones by pyrosequencing. The sensitivity and specificity of the criteria revised by pyrosequencing have been successfully improved by using CpG sites having the largest diagnostic

impact on each BAC clone. It has been validated that screening by BAMCA, which has an ability for detecting any tendency for coordinated regulation of DNA methylation at multiple CpG sites in the entire BAC region, followed by revision using pyrosequencing, is a promising approach for carcinogenetic risk estimation. Pyrosequencing can be performed using a very small amount of degraded DNA extracted from liver biopsy specimens. In other words, unless another approach such as pyrosequencing is used to validate BAMCA data, risk assessment of liver biopsy specimens based only on BAMCA is premature. We now intend to validate the reliability of such risk estimation prospectively using liver biopsy specimens obtained prior to interferon therapy from a large cohort of patients with HBV or HCV infection.

Urothelial carcinomas are clinically remarkable because of their multicentricity owing to the 'field effect', whereby carcinogenic agents in the urine cause malignant transformation of multiple urothelial cells [66]. Even noncancerous urothelia showing no remarkable histological features obtained from patients with UCs can be considered to be at the precancerous stage, because they may be exposed to carcinogens in the urine. On the other hand, UCs are classified as superficial papillary carcinomas or nodular invasive carcinomas according to their configuration (FIGURE 4A) [66]. Superficial papillary carcinomas usually remain noninvasive, although patients need to undergo repeated urethrocystoscopic resection because of recurrences. By contrast, the clinical outcome of nodular invasive carcinoma is poor. In our previous study, accumulation of DNA methylation on C-type CpG islands associated with DNMT1 overexpression was observed even in noncancerous urothelia obtained from patients with UCs, and was further increased especially in nodular invasive carcinomas [67,68]. These previous data suggest that carcinogenetic risk estimation of UCs based on DNA methylation status might be a promising strategy.

We carefully took the tissue specimens from the surface of elevated UC lesions to avoid contamination with noncancerous urothelial and stromal cells. Principal component analysis based on BAMCA data revealed that stepwise DNA methylation alterations from 17 samples of noncancerous urothelia obtained from patients with UCs to 40 samples of UCs, in comparison with 18 samples of normal urothelia, occurred in a genome-wide manner [55]. We then performed unsupervised 2D hierarchical clustering analysis based on BAMCA data for noncancerous urothelia. The examined patients with UCs were clustered into two subclasses, clusters A_{NU} and B_{NU}. The incidence of invasive UCs (pT2 or more) was significantly higher in patients belonging to cluster B_{NU} defined on the basis of DNA methylation status in their noncancerous urothelia in comparison to cluster A_{NU} [55]. Moreover, Wilcoxon test identified the BAC clones whose signal ratios differed significantly between noncancerous urothelia obtained from patients with superficial UCs (pTa and pT1) and noncancerous urothelia obtained from patients with invasive UCs (pT2 or more). DNA methylation profiles on such BAC clones of noncancerous urothelia obtained from patients with invasive UCs were inherited by the invasive UCs themselves (FIGURE 4B) [55]. DNA methylation alterations that were correlated with the development of more malignant invasive cancers were already accumulated in noncancerous urothelia.

To estimate the degree of carcinogenetic risk based on DNA methylation profiles in noncancerous urothelia, 83 BAC clones whose signal ratios discriminated noncancerous urothelia obtained from patients with UCs from normal urothelia with a sensitivity and specificity of 75% or more than 75% were identified. We established the criteria for carcinogenetic risk estimation by combining the cutoff values of the signal ratios for these 83 BAC clones [55]. We are currently attempting to develop a methodology for assessing the tendency of DNA methylation in the 83 BAC regions in urine samples to make such risk estimation applicable to healthy individuals. If it proves possible to identify individuals who are at high risk of urothelial carcinogenesis, then strategies for the prevention or early detection of UCs, such as smoking cessation or repeated urine cytology examinations, might be applicable.

Approximately 10–30% of patients with UCs of the renal pelvis and ureter develop intravesical metachronous UCs after nephroureterectomy [69]. Therefore, such patients need to undergo repeated urethrocystoscopic examinations to detect intravesical metachronous UCs. To decrease the need for invasive urethrocystoscopic examinations and assist close follow-up of such patients after nephroureterectomy, indicators for intravesical metachronous UCs have been needed. Since such metachronous UC originates from the noncancerous urothelium of the urinary bladder, we focused on the DNA methylation status of noncancerous urothelia, which may be exposed to the same carcinogens

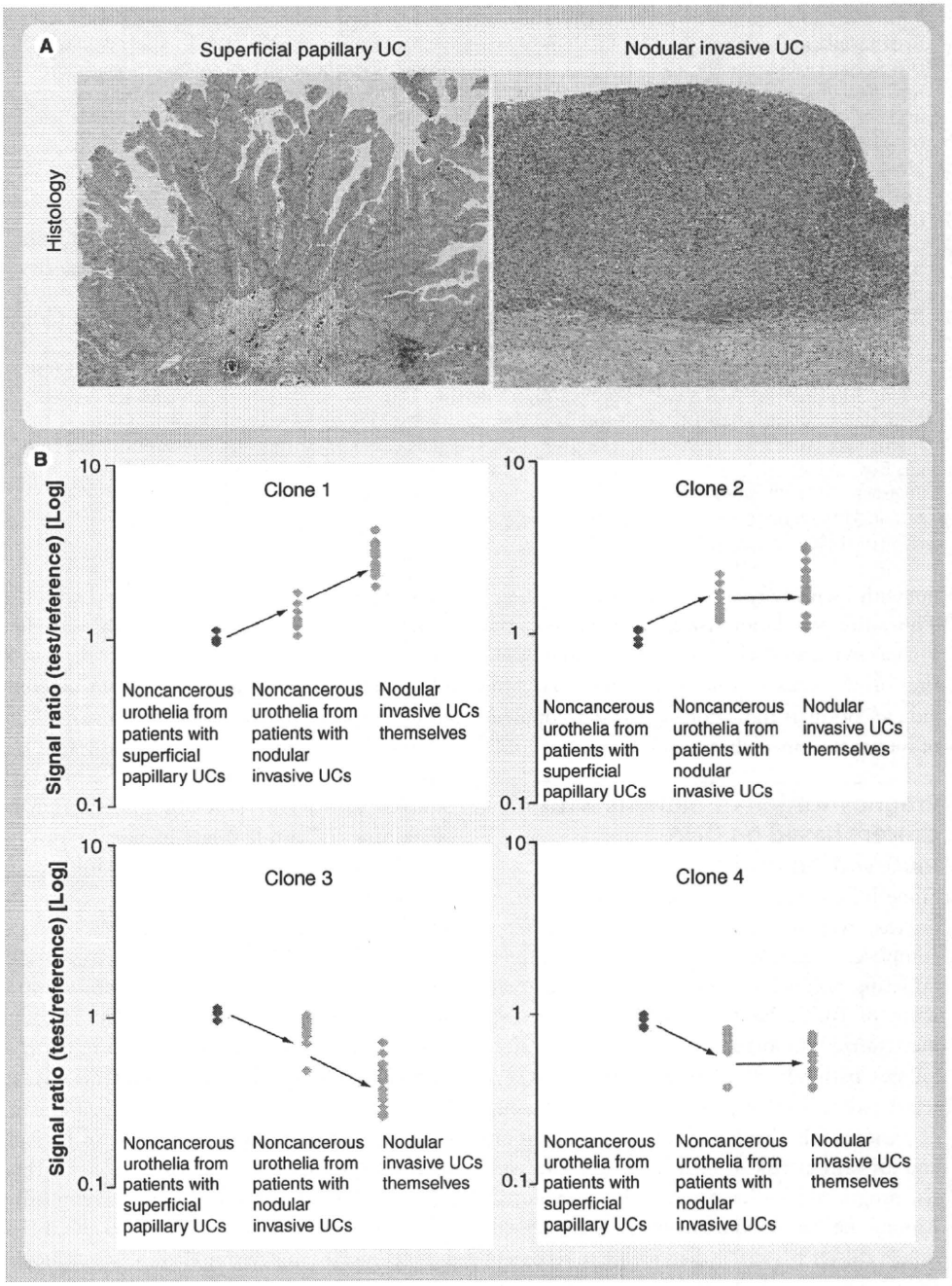

Figure 4. Significance of DNA methylation alterations at precancerous stages during urothelial carcinogenesis. For legend please see facing page.

in the urine, obtained by nephroureterectomy from patients with UCs of the renal pelvis or ureter. Unsupervised 2D hierarchical clustering analysis based on BAMCA data for noncancerous urothelia obtained from patients with UCs of the renal pelvis or ureter was able to group the examined patients into two subclasses, clusters A_{NP} and B_{NP}. The patients in cluster B_{NP} frequently developed intravesical metachronous UCs, whereas none belonging to cluster A_{NP} did so [55], indicating that DNA methylation profiles of noncancerous urothelia obtained by nephroureterectomy from patients with UCs of the renal pelvis or ureter are correlated with the risk of intravesical metachronous UC development. We identified nine BAC clones whose signal ratios discriminated noncancerous urothelia obtained from patients with UCs of the renal pelvis or ureter who developed intravesical metachronous UC after nephroureterectomy from noncancerous urothelia obtained from patients with UCs of the renal pelvis or ureter who did

Figure 4. Significance of DNA methylation alterations at precancerous stages during urothelial carcinogenesis. (A) Histological features of superficial papillary UC and nodular invasive UC. Superficial papillary carcinomas usually remain noninvasive, although patients need to undergo repeated urethrocystoscopic resection because of recurrences. By contrast, the clinical outcome of nodular invasive carcinomas is poor. **(B)** Scattergrams of the signal ratios in noncancerous urothelia obtained from patients with superficial UCs, noncancerous urothelia obtained from patients with invasive UCs, and invasive UCs themselves. Wilcoxon test revealed that the signal ratios of 131 bacterial artificial chromosome (BAC) clones differed significantly between noncancerous urothelia obtained from patients with superficial UCs and noncancerous urothelia obtained from patients with invasive UCs. If the average signal ratios in noncancerous urothelia obtained from patients with invasive UCs were significantly higher than those in noncancerous urothelia obtained from patients with superficial UCs (67 BAC clones), the average signal ratios in invasive UCs themselves were even higher than (42 BAC clones such as clone 1), or not significantly different from (25 BAC clones such as clone 2), those in noncancerous urothelia obtained from patients with invasive UCs without exception. If the average signal ratios in noncancerous urothelia obtained from patients with invasive UCs were significantly lower than those in noncancerous urothelia obtained from patients with superficial UCs (64 BAC clones), the average signal ratios in invasive UCs themselves were even lower than (38 BAC clones such as clone 3), or not significantly different from (26 BAC clones such as clone 4), those in noncancerous urothelia obtained from patients with invasive UCs without exception. Therefore, DNA methylation profiles of noncancerous urothelia obtained from patients with invasive UCs were inherited by the invasive UCs themselves.
UC: Urothelial carcinoma.

not with a sensitivity and specificity of 100% [55]. Thus, after validation using other technologies such as pyrosequencing, a combination of CpG sites on the present nine BAC clones may provide an optimal indicator for the development of intravesical metachronous UC.

Prognostication of patients with cancers based on DNA methylation profiles

Some RCCs relapse and metastasize to distant organs, even if resection has been considered complete. Recently, immunotherapy and novel targeting agents have been developed for treatment of RCC. However, unless relapsed or metastasized tumors are diagnosed early by close follow-up, the effectiveness of any therapy is very restricted. Therefore, to assist close follow-up of patients who have undergone nephrectomy and are still at risk of recurrence and metastasis, prognostic indicators have been explored. Among the examined patients in the abovementioned cluster B_{TK}, 38% died owing to recurrent RCCs, whereas only 2.3% of the patients in cluster A_{TK} died. Multivariate analysis revealed that our clustering was a predictor of recurrence and was independent of histological grade, macroscopic configuration, vascular involvement and renal vein tumor thrombi [60]. We were able to set the cutoff values of the signal ratios for 14 BAC clones to determine whether or not patients in this cohort belonged to cluster B_{TK} with a sensitivity and specificity of 100% [60].

To establish criteria for prognostication of patients with HCCs, in the learning cohort, HCC samples obtained from patients who had survived more than 4 years after hepatectomy and HCC samples obtained from patients who had suffered recurrence within 6 months and died within a year after hepatectomy were defined as a favorable-outcome group and a poor-outcome group, respectively. Wilcoxon test revealed that the signal ratios of 41 BAC clones differed significantly between the two groups (n = 19). We established the criteria for prognostication by combining the cutoff values of signal ratios for the 41 BAC clones (FIGURE 3B) [65]. Multivariate analysis revealed that satisfying the criteria for 32 or more BAC clones was a predictor of recurrence, and was independent of histological differentiation, portal vein tumor thrombi, intrahepatic metastasis and multicentricity [65]. The cancer-free and overall survival rates of patients with HCCs in the validation cohort (n = 44) satisfying the criteria for 32 or more BAC clones were significantly lower than those of patients with HCCs satisfying the criteria for less than 32 BAC clones [65]. Such prognostication using biopsy or hepatectomy specimens may be able to assist clinicians in devising therapeutic strategies for patients with insufficient liver function.

Recently, new forms of systemic chemotherapy and targeted therapy have been developed for treatment of UCs. In order to start adjuvant systemic chemotherapy immediately in patients who have undergone surgery and are still at high risk of recurrence and metastasis, prognostic indicators have been explored. It is expected that a combination of several CpG islands of tumor-related genes would be useful as epigenetic markers for prognostication of UCs [70]. In addition, when we applied BAMCA to UCs, unsupervised 2D hierarchical clustering analysis based on BAMCA data for UCs was

able to group the examined patients into two subclasses, clusters A_{TU} and B_{TU}. Among the patients belonging to cluster B_{TU}, 19% suffered recurrence after surgery, whereas none belonging to cluster A_{TU} did so [55]. Wilcoxon test revealed that the signal ratios of 20 BAC clones in UCs differed significantly between the patients who suffered recurrence after surgery and the patients who did not. The criteria for a combination of the 20 BAC clones were able to discriminate patients who suffered recurrence after surgery from patients who did not with a sensitivity and specificity of 100%, whereas a high histological grade, invasive growth (pT2 or more) and vascular or lymphatic involvement were incapable of such complete discrimination [55]. The reliability of such prognostication will need to be validated in a prospective study.

Future perspective

The incidence of DNA methylation alterations is generally high in various organs during multistage carcinogenesis. Since even subtle alterations of DNA methylation profiles at the precancerous stage are stably preserved on DNA double strands by covalent bonds, and these can be detected using highly sensitive methodology. Therefore, they may be better diagnostic indicators than mRNA and protein-expression profiles, which can be easily affected by the microenvironment of cancer cells or precursor cells. Genome-wide DNA methylation profiling can provide indicators for carcinogenetic risk estimation and prognostication using samples of urine, sputum and other body fluids, and also biopsy and surgically resected specimens. However, exploitation of diagnostic indicators can never be regarded as optimal, and it is expected that ongoing technical innovation and prospective validation will lead to further improvements of diagnostic sensitivity and specificity.

Patients with cancers are frequently clustered into subclasses showing both distinct genome-wide DNA methylation profiles and distinct clinicopathological characteristics (FIGURE 1B). Such clustering of cancers may provide clues for clarification of the molecular mechanisms establishing the distinct DNA methylation profiles of each cluster and the identification of target molecules for prevention and therapy in

Executive summary

Introduction

- Human cancer cells show a drastic change in DNA methylation status, that is overall DNA hypomethylation and regional DNA hypermethylation.
- DNA methylation alterations are known to result in altered expression of tumor-related genes and chromosomal instability in human cancers.

DNA methylation alterations during multistage carcinogenesis

- DNA methylation alterations play a significant role even at the precancerous stage, especially in association with chronic inflammation and persistent infection with viruses, such as hepatitis B virus or hepatitis C virus.
- DNA methyltransferase 1 overexpression in cancers is frequently correlated with accumulation of DNA methylation of tumor-related genes and poorer patient outcome.

Genome-wide DNA methylation analysis

- For genome-wide analysis, microarray platforms are used in combination with DNA methylation-sensitive restriction enzyme-based or antimethyl-cytosine antibody affinity techniques, and new generation sequencing technologies are also being introduced.
- Bacterial artificial chromosome array-based methylated CpG island amplification (BAMCA) may be suitable for overviewing the DNA methylation tendency of individual large regions among all chromosomes.

Genome-wide DNA methylation profiles at precancerous stages are inherited by cancers & determine tumor aggressiveness

- Distinct DNA methylation profiles in noncancerous tissue at the precancerous stage is basically inherited by the cancer developing in each individual patient.
- DNA methylation alterations at the precancerous stage, which may not occur randomly but may foster further epigenetic and genetic alterations, can generate more malignant cancers and even determine patient outcome.

Carcinogenetic risk estimation based on DNA methylation profiles

- On the basis of BAMCA data, criteria for estimation of the risk of hepatocellular carcinoma and urothelial carcinoma development have been established.

Prognostication of patients with cancers based on DNA methylation profiles

- On the basis of BAMCA data, criteria for the prognostication of patients with renal cell carcinomas, hepatocellular carcinomas and urothelial carcinomas have been established.

Future perspective

- Genome-wide DNA methylation profiling can provide indicators for carcinogenetic risk estimation and prognostication using samples of body fluids and tissue specimens.
- Based upon genome-wide DNA methylation profiling, translational epigenetics has come of age.

patients belonging to each cluster. Based upon of genome-wide DNA methylation profiling, translational epigenetics has clearly come of age.

Financial & competing interests disclosure

This study was supported by a Grant-in-Aid for the Third Term Comprehensive 10-Year Strategy for Cancer Control from the Ministry of Health, Labor and Welfare of Japan, a Grant-in-Aid for Cancer Research from the Ministry of Health, Labor and Welfare of Japan, a Grant from the New Energy and Industrial Technology Development Organization (NEDO), and the Program for Promotion of Fundamental Studies in Health Sciences of the National Institute of Biomedical Innovation (NiBio). The authors have no other relevant affiliations or financial involvement with any organization or entity with financial interest in or financial conflict with the subject matter or materials discussed in the manuscript apart from those disclosed.

No writing assistance was utilized in the production of this manuscript.

Ethical conduct of research

The authors state that they have obtained appropriate institutional review board approval or have followed the principles outlined in the Declaration of Helsinki for all human or animal experimental investigations. In addition, for investigations involving human subjects, informed consent has been obtained from the participants involved.

Bibliography

Papers of special note have been highlighted as:
- ▪ of interest

1 Jones PA, Baylin SB: The fundamental role of epigenetic events in cancer. *Nat. Rev. Genet.* 3, 415–428 (2002).

2 Jones PA, Baylin SB: The epigenomics of cancer. *Cell* 128, 683–692 (2007).

3 Sharma S, Kelly TK, Jones PA: Epigenetics in cancer. *Carcinogenesis* 31, 27–36 (2009).

4 Cedar H, Bergman Y: Linking DNA methylation and histone modification: patterns and paradigms. *Nat. Rev. Genet.* 10, 295–304 (2009).

5 Delcuve GP, Rastegar M, Davie JR: Epigenetic control. *J. Cell Physiol.* 219, 243–250 (2009).

6 Illingworth RS, Bird AP: CpG islands – 'a rough guide'. *FEBS Lett.* 583, 1713–1720 (2009).

7 Mohn F, Schubeler D: Genetics and epigenetics: stability and plasticity during cellular differentiation. *Trends. Genet.* 25, 129–136 (2009).

8 Yoshiura K, Kanai Y, Ochiai A, Shimoyama Y, Sugimura T, Hirohashi S: Silencing of the E-cadherin invasion-suppressor gene by CpG methylation in human carcinomas. *Proc. Natl Acad. Sci.* USA 92, 7416–7419 (1995).

▪ **E-cadherin tumor suppressor gene was shown to be silenced by DNA methylation, and the universality of a 'two-hit' mechanism involving DNA hypermethylation and loss of heterozygosity during carcinogenesis has been proposed.**

9 Baylin SB, Ohm JE: Epigenetic gene silencing in cancer – a mechanism for early oncogenic pathway addiction? *Nat. Rev. Cancer* 6, 107–116 (2006).

10 Shibata D: Inferring human stem cell behaviour from epigenetic drift. *J. Pathol.* 217, 199–205 (2009).

11 Ohm JE, McGarvey KM, Yu X *et al.*: A stem cell-like chromatin pattern may predispose tumor suppressor genes to DNA hypermethylation and heritable silencing. *Nat. Genet.* 39, 237–242 (2007).

12 Pogribny IP, Beland FA: DNA hypomethylation in the origin and pathogenesis of human diseases. *Cell Mol. Life Sci.* 66, 2249–2261 (2009).

13 Wong N, Lam WC, Lai PB, Pang E, Lau WY, Johnson PJ: Hypomethylation of chromosome 1 heterochromatin DNA correlates with q-arm copy gain in human hepatocellular carcinoma. *Am. J. Pathol.* 159, 465–471 (2001).

14 Nakagawa T, Kanai Y, Ushijima S, Kitamura T, Kakizoe T, Hirohashi S: DNA hypomethylation on pericentromeric satellite regions significantly correlates with loss of heterozygosity on chromosome 9 in urothelial carcinomas. *J. Urol.* 173, 243–246 (2005).

15 Okano M, Bell DW, Haber DA, Li E: DNA methyltransferases DNMT3a and Dnmt3b are essential for *de novo* methylation and mammalian development. *Cell* 99, 247–257 (1999).

16 Saito Y, Kanai Y, Sakamoto M, Saito H, Ishii H, Hirohashi S: Overexpression of a splice variant of DNA methyltransferase 3b, DNMT3b4, associated with DNA hypomethylation on pericentromeric satellite regions during human hepatocarcinogenesis. *Proc. Natl Acad. Sci. USA* 99, 10060–10065 (2002).

▪ **Overexpression of an inactive splice variant of DNMT3b, which competes with the major splice variant for targeting to pericentromeric satellite regions, has been proposed as one of the molecular mechanisms for chromosomal instability during hepatocarcinogenesis.**

17 Laird PW: The power and the promise of DNA methylation markers. *Nat. Rev. Cancer* 3, 253–266 (2003).

18 Issa JP, Kantarjian HM: Targeting DNA methylation. *Clin. Cancer Res.* 15, 3938–3946 (2009).

19 Swanton C, Caldas C: Molecular classification of solid tumours: towards pathway-driven therapeutics. *Br. J. Cancer* 100, 1517–1522 (2009).

20 Kanai Y, Hirohashi S: Alterations of DNA methylation associated with abnormalities of DNA methyltransferases in human cancers during transition from a precancerous to a malignant state. *Carcinogenesis* 28, 2434–2442 (2007).

▪ **Results of empirical analysis of DNA methylation status and DNA methyltransferase abnormalities in clinical tissue samples in connection with the clinicopathological parameters of human cancers have been reviewed.**

21 Kanai Y: Alterations of DNA methylation and clinicopathological diversity of human cancers. *Pathol. Int.* 58, 544–558 (2008).

22 Kanai Y: Genome-wide DNA methylation profiles in precancerous conditions and cancers. *Cancer Sci.* 101, 36–45 (2010).

23 Kanai Y, Ushijima S, Tsuda H, Sakamoto M, Sugimura T, Hirohashi S: Aberrant DNA methylation on chromosome 16 is an early event in hepatocarcinogenesis. *Jpn. J. Cancer Res.* 87, 1210–1217 (1996).

▪ **One of the earliest reports of DNA methylation alterations at the precancerous stage, especially in noncancerous liver tissue showing chronic hepatitis or cirrhosis, which are widely considered to be precancerous conditions for hepatocellular carcinomas.**

24 Kanai Y, Hui AM, Sun L *et al.*: DNA hypermethylation at the D17S5 locus and reduced HIC-1 mRNA expression are associated with hepatocarcinogenesis. *Hepatology* 29, 703–709 (1999).

25 Kondo Y, Kanai Y, Sakamoto M, Mizokami M, Ueda R, Hirohashi S: Genetic instability and aberrant DNA methylation in chronic hepatitis and cirrhosis – a comprehensive study of loss of heterozygosity and microsatellite instability at 39 loci and DNA hypermethylation on 8 CpG islands in microdissected specimens from patients with hepatocellular carcinoma. *Hepatology* 32, 970–979 (2000).

26 Etoh T, Kanai Y, Ushijima S *et al.*: Increased DNA methyltransferase 1 (DNMT1) protein expression correlates significantly with poorer tumor differentiation and frequent DNA hypermethylation of multiple CpG islands in gastric cancers. *Am. J. Pathol.* 164, 689–699 (2004).

27 Wentzensen N, Sherman ME, Schiffman M, Wang SS: Utility of methylation markers in cervical cancer early detection: appraisal of the state-of-the-science. *Gynecol. Oncol.* 112, 293–299 (2009).

28 Ushijima T: Epigenetic field for cancerization. *J. Biochem. Mol. Biol.* 40, 142–150 (2007).

29 Eguchi K, Kanai Y, Kobayashi K, Hirohashi S: DNA hypermethylation at the D17S5 locus in non-small cell lung cancers: its association with smoking history. *Cancer Res.* 57, 4913–4915 (1997).

30 Toyota M, Ahuja N, Ohe-Toyota M, Herman JG, Baylin SB, Issa JP: CpG island methylator phenotype in colorectal cancer. *Proc. Natl Acad. Sci. USA* 96, 8681–8686 (1999).

31 Kanai Y, Ushijima S, Hui AM *et al.*: The E-cadherin gene is silenced by CpG methylation in human hepatocellular carcinomas. *Int. J. Cancer* 71, 355–359 (1997).

32 Saito Y, Kanai Y, Sakamoto M, Saito H, Ishii H, Hirohashi S: Expression of mRNA for DNA methyltransferases and methyl-CpG-binding proteins and DNA methylation status on CpG islands and pericentromeric satellite regions during human hepatocarcinogenesis. *Hepatology* 33, 561–568 (2001).

33 Saito Y, Kanai Y, Nakagawa T *et al.*: Increased protein expression of DNA methyltransferase (DNMT) 1 is significantly correlated with the malignant potential and poor prognosis of human hepatocellular carcinomas. *Int. J. Cancer* 105, 527–532 (2003).

34 Peng DF, Kanai Y, Sawada M *et al.*: Increased DNA methyltransferase 1 (DNMT1) protein expression in precancerous conditions and ductal carcinomas of the pancreas. *Cancer Sci.* 96, 403–408 (2005).

35 Peng DF, Kanai Y, Sawada M *et al.*: DNA methylation of multiple tumor-related genes in association with overexpression of DNA methyltransferase 1 (DNMT1) during multistage carcinogenesis of the pancreas. *Carcinogenesis* 27, 1160–1168 (2006).

36 Ooi SK, O'Donnell AH, Bestor TH: Mammalian cytosine methylation at a glance. *J. Cell Sci.* 122, 2787–2791 (2009).

37 Chuang LS, Ian HI, Koh TW, Ng HH, Xu G, Li BF: Human DNA-(cytosine-5) methyltransferase-PCNA complex as a target for p21WAF1. *Science* 277, 1996–2000 (1997).

38 Kanai Y, Ushijima S, Kondo Y, Nakanishi Y, Hirohashi S: DNA methyltransferase expression and DNA methylation of CpG islands and peri-centromeric satellite regions in human colorectal and stomach cancers. *Int. J. Cancer* 91, 205–212 (2001).

39 Damiani LA, Yingling CM, Leng S, Romo PE, Nakamura J, Belinsky SA: Carcinogen-induced gene promoter hypermethylation is mediated by DNMT1 and causal for transformation of immortalized bronchial epithelial cells. *Cancer Res.* 68, 9005–9014 (2008).

40 Liao X, Siu MK, Chan KY *et al.*: Hypermethylation of RAS effector related genes and DNA methyltransferase 1 expression in endometrial carcinogenesis. *Int. J. Cancer* 123, 296–302 (2008).

41 Hino R, Uozaki H, Murakami N *et al.*: Activation of DNA methyltransferase 1 by EBV latent membrane protein 2A leads to promoter hypermethylation of *PTEN* gene in gastric carcinoma. *Cancer Res.* 69, 2766–2774 (2009).

42 Gao P, Yang X, Xue YW *et al.*: Promoter methylation of glutathione *S*-transferase pi1 and multidrug resistance gene 1 in bronchioloalveolar carcinoma and its correlation with DNA methyltransferase 1 expression. *Cancer* 115, 3222–3232 (2009).

43 Lin RK, Hsieh YS, Lin P *et al.*: The tobacco-specific carcinogen NNK induces DNA methyltransferase 1 accumulation and tumor suppressor gene hypermethylation in mice and lung cancer patients. *J. Clin. Invest.* 120, 521–532 (2010).

44 Eads CA, Danenberg KD, Kawakami K, Saltz LB, Danenberg PV, Laird PW: CpG island hypermethylation in human colorectal tumors is not associated with DNA methyltransferase overexpression. *Cancer Res.* 59, 2302–2306 (1999).

45 Park HJ, Yu E, Shim YH: DNA methyltransferase expression and DNA hypermethylation in human hepatocellular carcinoma. *Cancer Lett.* 233, 271–278 (2006).

46 Kondo Y, Shen L, Suzuki S *et al.*: Alterations of DNA methylation and histone modifications contribute to gene silencing in hepatocellular carcinomas. *Hepatol. Res.* 37, 974–983 (2007).

47 Estecio MR, Yan PS, Ibrahim AE *et al.*: High-throughput methylation profiling by MCA coupled to CpG island microarray. *Genome Res.* 17, 1529–1536 (2007).

48 Estecio MR, Issa JP: Tackling the methylome: recent methodological advances in genome-wide methylation profiling. *Genome Med.* 1, 106 (2009).

49 Bibikova M, Fan JB: GoldenGate assay for DNA methylation profiling. *Methods Mol. Biol.* 507, 149–163 (2009).

50 Gunderson KL: Whole-genome genotyping on bead arrays. *Methods Mol. Biol.* 529, 197–213 (2009).

51 Eid J, Fehr A, Gray J *et al.*: Real-time DNA sequencing from single polymerase molecules. *Science* 323, 133–138 (2009).

52 Maekita T, Nakazawa K, Mihara M *et al.*: High levels of aberrant DNA methylation in *Helicobacter pylori*-infected gastric mucosae and its possible association with gastric cancer risk. *Clin. Cancer Res.* 12, 989–995 (2006).

53 Clark SJ: Action at a distance: epigenetic silencing of large chromosomal regions in carcinogenesis. *Hum. Mol. Genet.* 16(Spec. No. 1), R88–R95 (2007).

54 Inazawa J, Inoue J, Imoto I: Comparative genomic hybridization (CGH)-arrays pave the way for identification of novel cancer-related genes. *Cancer Sci.* 95, 559–563 (2004).

55 Nishiyama N, Arai E, Chihara Y *et al.*: Genome-wide DNA methylation profiles in urothelial carcinomas and urothelia at the precancerous stage. *Cancer Sci.* 101, 231–240 (2010).

▪ **Indicators for risk estimation of the development of urothelial carcinomas and prognostication of patients with urothelial carcinomas have been established based on bacterial artificial chromosome array-based methylated CpG island amplification (BAMCA) data.**

56 Misawa A, Inoue J, Sugino Y *et al.*: Methylation-associated silencing of the nuclear receptor *1I2* gene in advanced-type neuroblastomas, identified by bacterial artificial chromosome array-based methylated CpG island amplification. *Cancer Res.* 65, 10233–10242 (2005).

57 Tanaka K, Imoto I, Inoue J *et al.*: Frequent methylation-associated silencing of a candidate tumor-suppressor, CRABP1, in esophageal squamous-cell carcinoma. *Oncogene* 26, 6456–6468 (2007).

58 Sugino Y, Misawa A, Inoue J *et al.*: Epigenetic silencing of prostaglandin E receptor 2 (PTGER2) is associated with progression of neuroblastomas. *Oncogene* 26, 7401–7413 (2007).

59 McRonald FE, Morris MR, Gentle D *et al.*: CpG methylation profiling in VHL related and VHL unrelated renal cell carcinoma. *Mol. Cancer* 8, 31–41 (2009).

60 Arai E, Ushijima S, Fujimoto H *et al.*: Genome-wide DNA methylation profiles in both precancerous conditions and clear cell renal cell carcinomas are correlated with malignant potential and patient outcome. *Carcinogenesis* 30, 214–221 (2009).

- **Genome-wide DNA methylation profiles in precancerous conditions of the kidney have been shown to be inherited by clear cell renal cell carcinomas developing in each individual patient, and to determine tumor aggressiveness and patient outcome.**

61 Arai E, Kanai Y, Ushijima S, Fujimoto H, Mukai K, Hirohashi S: Regional DNA hypermethylation and DNA methyltransferase (DNMT) 1 protein overexpression in both renal tumors and corresponding nontumorous renal tissues. *Int. J. Cancer* 119, 288–296 (2006).

62 Arai E, Ushijima S, Tsuda H *et al.*: Genetic clustering of clear cell renal cell carcinoma based on array-comparative genomic hybridization: its association with DNA methylation alteration and patient outcome. *Clin. Cancer Res.* 14, 5531–5539 (2008).

63 Lee HS, Kim BH, Cho NY *et al.*: Prognostic implications of and relationship between CpG island hypermethylation and repetitive DNA hypomethylation in hepatocellular carcinoma. *Clin. Cancer Res.* 15, 812–820 (2009).

64 Moribe T, Iizuka N, Miura T *et al.*: Methylation of multiple genes as molecular markers for diagnosis of a small, well-differentiated hepatocellular carcinoma. *Int. J. Cancer* 125, 388–397 (2009).

65 Arai E, Ushijima S, Gotoh M *et al.*: Genome-wide DNA methylation profiles in liver tissue at the precancerous stage and in hepatocellular carcinoma. *Int. J. Cancer* 125, 2854–2862 (2009).

- **Indicators for carcinogenetic risk estimation in chronically diseased liver, and prognostication of patients with hepatocellular carcinomas, have been established based on BAMCA data.**

66 Kakizoe T: Development and progression of urothelial carcinoma. *Cancer Sci.* 97, 821–828 (2006).

67 Nakagawa T, Kanai Y, Ushijima S, Kitamura T, Kakizoe T, Hirohashi S: DNA hypermethylation on multiple CpG islands associated with increased DNA methyltransferase DNMT1 protein expression during multistage urothelial carcinogenesis. *J. Urol.* 173, 1767–1771 (2005).

68 Nakagawa T, Kanai Y, Saito Y, Kitamura T, Kakizoe T, Hirohashi S: Increased DNA methyltransferase 1 protein expression in human transitional cell carcinoma of the bladder. *J. Urol.* 170, 2463–2466 (2003).

69 Manabe D, Saika T, Ebara S *et al.*: Comparative study of oncologic outcome of laparoscopic nephroureterectomy and standard nephroureterectomy for upper urinary tract transitional cell carcinoma. *Urology* 69, 457–461 (2007).

70 Kim WJ, Kim YJ: Epigenetic markers as promising prognosticators for bladder cancer. *Int. J. Urol.* 16, 17–22 (2009).

DOI 10.1002/prca.200900172 *Proteomics Clin. Appl.* 2010, *4*, 560–567

RESEARCH ARTICLE

Peroxiredoxin 2 as a chemotherapy responsiveness biomarker candidate in osteosarcoma revealed by proteomics

Kazutaka Kikuta[1,2], Naobumi Tochigi[3], Shigeru Saito[1,4], Tadakazu Shimoda[3], Hideo Morioka[2], Yoshiaki Toyama[2], Ako Hosono[5], Yoshiyuki Suehara[6], Yasuo Beppu[7], Akira Kawai[7], Setsuo Hirohashi[1] and Tadashi Kondo[1]

[1] Proteome Bioinformatics Project, National Cancer Center Research Institute, Tokyo, Japan
[2] Department of Orthopedic Surgery, Keio University School of Medicine, Tokyo, Japan
[3] Diagnosis Pathology Division, National Cancer Center Hospital, Tokyo, Japan
[4] Chemistry and Bioinformatics Department, Infocom Corporation, Tokyo, Japan
[5] Pediatric Oncology Division, National Cancer Center Hospital, Tokyo, Japan
[6] Department of Orthopedic Surgery, Juntendo University School of Medicine, Tokyo, Japan
[7] Orthopedic Surgery Division, National Cancer Center Hospital, Tokyo, Japan

Received: August 19, 2009
Revised: January 24, 2010
Accepted: January 24, 2010

Purpose: We aimed to identify novel chemotherapy responsiveness biomarkers for osteosarcoma (OS) by investigating the global protein expression profile of 12 biopsy samples from OS patients.

Experimental design: Six patients were classified as good responders and six as poor responders, according to the Huvos grading system. The protein expression profiles obtained by 2-D DIGE consisted of 2250 protein spots.

Results: Among them, we identified 55 protein spots whose intensity was significantly different (Bonferroni adjusted p-value < 0.01) between the two patient groups. Mass spectrometric protein identification demonstrated that the 55 spots corresponded to 38 distinct gene products including peroxiredoxin 2 (PRDX 2). Use of a specific antibody against PRDX 2 confirmed the differential expression of PRDX 2 between good and poor responders, while PRDX 2 levels as measured by Western blotting correlated highly with their corresponding 2-D DIGE values. The predictive value of PRDX 2 expression was further confirmed by examining an additional four OS cases using Western blotting.

Conclusions and clinical relevance: These results establish PRDX 2 as a candidate for chemotherapy responsiveness marker in OS. Measuring PRDX 2 in biopsy samples before treatment may contribute to more effective management of OS.

Keywords:
2-D DIGE / Chemotherapy / Osteosarcoma / Peroxiredoxin 2

1 Introduction

Osteosarcoma (OS) is the most common primary malignant bone tumor in children and adolescents [1, 2]. In the mid-1970s, Rosen *et al.* noted that the response to the initial chemotherapy for OS was predictive of long-term outcome [3]; others have subsequently confirmed this finding [4, 5]. During the past three decades, the standard treatment for OS has been surgery and neo- and adjuvant chemotherapy. Chemotherapy has improved the cure rate of patients with localized OS from 15 to 20% achieved with surgery alone to approximately 70% [6]. However, OS patients whose tumors respond poorly to chemotherapy are at a higher risk of relapse and poor outcome, and chemotherapy response has always been the most important, and most consistently reported, predictor for survival [7–13]. Therefore, it is

Correspondence: Dr. Tadashi Kondo, Proteome Bioinformatics Project, National Cancer Center Research Institute, 5-1-1 Tsukiji, Chuo-ku, Tokyo 104-0045, Japan
E-mail: takondo@ncc.go.jp
Fax: +81-3-357-5298

Abbreviation: ADR, doxorubicin; **CDDP,** cisplatin; **IFO,** ifosfamide; **OS,** osteosarcoma; **PRDX 2,** peroxiredoxin 2

imperative to identify chemotherapy responsiveness biomarkers at the time of diagnosis and prior to the initiation of therapy to detect chemotherapy-resistant tumors and to modify the treatment regimen appropriately.

Response to chemotherapy following the induction chemotherapy is evaluated using the Huvos grading system, where the levels of tumor necrosis achieved reflect the effectiveness of the given chemotherapy. Patients with $\geq 90\%$ tumor necrosis following induction therapy are classified as good responders and patients with $<90\%$ tumor necrosis as poor responders [2]. Although this grading system is a powerful predictor of chemotherapy responsiveness, it can only be determined after chemotherapy.

In recent years, high-throughput screening technologies such as cDNA microarray technology have been used to develop biomarkers to predict the response to chemotherapy. A small number of comprehensive studies using these technologies suggested the presence of a chemotherapy resistance signature before treatment and identified a number of genes that were involved in the process of chemotherapy responsiveness in OS [14, 15]. However, none of the identified genes and signatures has been used in a clinical setting.

Emerging technologies that examine the overall features of the expressed proteins, namely proteomics, have identified many candidate proteins associated with early diagnosis [16], differential diagnosis [17], prognosis [18, 19], and response to chemotherapy [20] in various diseases. However, there is no proteomic study on predicting the response to chemotherapy in OS to date.

In this study, using biopsy samples taken prior to therapy, we found that peroxiredoxin 2 (PRDX 2) expression significantly correlated with the response to chemotherapy resistance of OS, and thus establishing PRDX 2 expression as a novel biomarker in OS.

2 Materials and methods

2.1 Patients and clinical information

Sixteen OS cases, including 12 cases used for protein expression profiling and Western blotting and four cases used in the validation study using Western blotting, were diagnosed and treated in the National Cancer Center Hospital between 2003 and 2008. Biopsy samples prior to any treatment were obtained from all 16 OS cases. The clinical information of the patients is summarized in Table 1. These 16 cases were diagnosed as conventional type OS that had developed in the extremities, in younger patients. All cases were treated with the identical induction chemotherapy protocol that included ifosfamide (IFO), cisplatin (CDDP) and doxorubicin (ADR), all of which are key drugs in the recent protocols. According to the Huvos grading system [2], chemotherapy responsiveness was defined based on histological observations on the resected specimens. Using the Huvos grading system, the cases where a tumor contained at least 90% of necrotic regions were defined as good responders (Huvos 3/4), while cases in which the necrotic regions covered $<90\%$ of the tumor area examined (Huvos 1/2) were defined as poor responders. Samples were snap frozen in liquid nitrogen and stored at –80°C until use. This project was approved by the ethical review board of the National Cancer Center, after signed informed consent was obtained from all patients. All cases were reviewed and histopathologically diagnosed by certified pathologists (N. T. and T. S.).

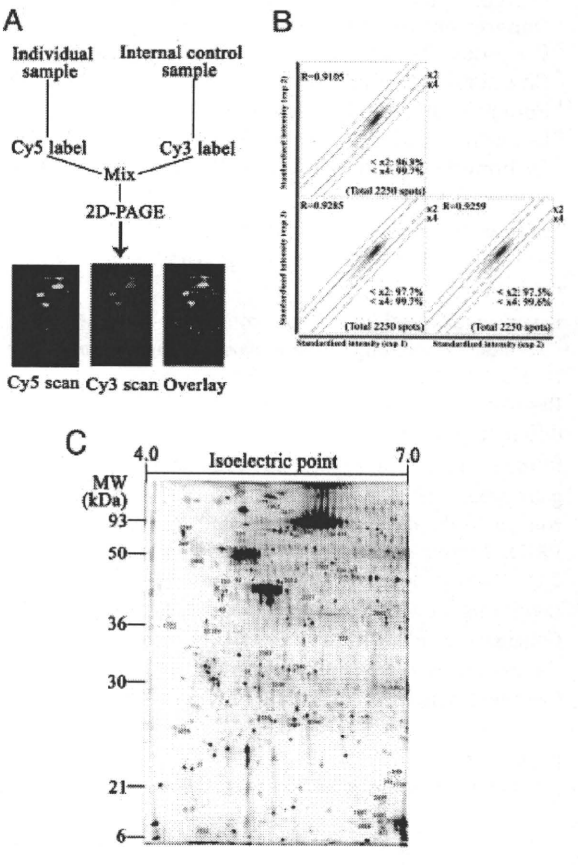

Figure 1. Identification of proteins differentially expressed in OS. (A) Schematic workflow of sample preparation for quantitative analysis. Protein lysates are labeled with fluorescent dyes of different wavelengths of excitation and emission. Cy3-labeled samples are simultaneously mixed and divided into Cy5-labeled samples. Then, the Cy3- and Cy5-labeled lysates are co-separated by 2-D DIGE. The gel is scanned at two wavelengths, each specific for each dye. (B) Scattergram of the expression profile of OS tissues. Comparison of data from three independent experiments revealed the high reproducibility of protein expression profiling. (C) Representative 2-D image of proteins detected in OS tissues. The 55 spots identified in this study are circled and numbered. The spot numbers correspond to those in Fig. 2, Table 2, and Supporting information Table 1.

2.2 Protein expression profiling

Frozen samples were crushed to powder with a Multi-beads shocker (Yasui Kikai, Osaka, Japan) with liquid nitrogen. The frozen powder was then treated with urea lysis buffer (6 M urea, 2 M thiourea, 3% CHAPS, 1% Triton X-100). After centrifugation at 15 000 rpm for 30 min, the supernatant was recovered and used in the subsequent protein expression studies.

2-D DIGE was performed as described previously [21]. In brief, the internal control sample was prepared by mixing a portion of all individual samples. Five micrograms of the internal control sample and each of the individual samples were labeled with Cy3 and Cy5, respectively (CyDye DIGE Fluor saturation dye, GE Healthcare Biosciences, Uppsala, Sweden) according to the manufacturer's instructions. The differently labeled protein samples were mixed and separated by 2-D gel electrophoresis. The first-dimension separation was achieved using IPG DryStrip gels (24 cm length, p*I* range between 4 and 7, GE Healthcare Biosciences). The second-dimension separation was achieved by SDS-PAGE on large-format gels (38 cm length, Bio-craft, Itabashi, Tokyo, Japan) [21]. The gels were scanned using laser scanners (Tyhoon Trio, GE Healthcare Biosciences) at appropriate wavelengths (Fig. 1A). For all spots, the intensity of the Cy5 image was normalized by that of the Cy3 image in the identical gel so that gel-to-gel differences were compensated, using the Progenesis PG240 software (Nonlinear Dynamics, Newcastle upon Tyne, UK). System reproducibility was verified by comparing the protein profiles obtained from three independent separations of the same sample (case 1, Table 1). Scatter plot analysis revealed that the standardized intensity of more than 96.8% of the spots ranged within a two-fold difference (Fig. 1B, $R = 0.9105$).

2.3 Data analysis

The numerical data in the XML files were imported to Expressionist software (GeneData, Basel, Switzerland) for scatter-plotting and hierarchical clustering. The Kruskal–Wallis test and Bonferroni adjustment were used to identify the protein spots that showed different intensities between the good and the poor responders.

2.4 Protein identification by mass spectrometry

The proteins corresponding to the detected spots were identified using mass spectrometry, according to our previous report [21]. In brief, 100 μg of Cy5- or Cy3-labeled proteins were separated by 2-D PAGE, recovered as gel plugs and digested with modified trypsin (Promega, Madison, WI, USA). The trypsin digests were subjected to LC (Paradigm MS4 dual solvent delivery system, Michrom BioResources, Auburn, CA) and MS using a Finnigan LTQ linear ion trap mass spectrometer (Thermo Electron, San Jose, CA, USA) equipped with a nano-electrospray ion source (AMR, Megro, Tokyo, Japan). The MASCOT software

Table 1. Clinicopathologic features of the cases frozen samples of which were examined by proteomics

Case no.	Age (years)	Sex	Histological subtype	Site	Huvos grading	Metastasis at diagnosis	Preoperation chemotherapy agents	Dose of chemotherapy IFO (g)/CDDP (mg)/ADR (mg)
1	38	Female	Osteoblastic	Distal femur	3	–	IFO, CDDP/ADR	14/100/60
2	16	Male	Fibroblastic	Proximal tibia	1	–	IFO, CDDP/ADR	14/120/60
3	14	Male	Osteoblastic	Distal femur	1	Metastasis (skip)	IFO, CDDP/ADR	14/120/60
4	23	Female	Osteoblastic	Proximal humerus	1	Metastasis (lung)	IFO, CDDP/ADR	14/120/60
5	11	Male	Osteoblastic	Proximal tibia	1	–	IFO, CDDP/ADR	14/120/60
6	25	Male	Osteoblastic	Diaphesis of humerus	3	–	IFO, CDDP/ADR	16/120/60
7	15	Female	Teleangiectatic	Distal femur	4	–	IFO, CDDP/ADR	14/120/60
8	13	Male	Osteoblastic	Proximal tibia	1	–	IFO, CDDP/ADR	14/120/60
9	18	Male	Osteoblastic	Distal tibia	3	–	IFO, CDDP/ADR	14/120/60
10	16	Male	Chondroblastic	Proximal tibia	4	–	IFO, CDDP/ADR	14/120/60
11	14	Male	Chondroblastic	Proximal femur	1	Metastasis (lung)	IFO, CDDP/ADR	14/120/60
12	8	Male	Osteoblastic	Proximal humerus	3	–	IFO, CDDP/ADR	14/120/60
13	20	Male	Osteoblastic	Distal femur	3	–	IFO, CDDP/ADR	14/120/60
14	7	Female	Osteoblastic	Distal femur	3	–	IFO, CDDP/ADR	14/120/60
15	11	Female	Chondroblastic	distal femur	1	–	IFO[a)]	14[a)]
16	14	Male	Osteoblastic	distal femur	1	–	IFO, CDDP/ADR	14/120/60

a) Severe myelosuppression and could not continue IFO, CDDP/ADR protocol.

(version 2.1, Matrix Science, London, UK) was used to search for the mass of the peptide ion peaks against the Swiss-Prot database (*Homo sapiens*, 12867 sequence in Sprot_47.8 fasta file).

2.5 Western blotting

Protein samples were separated by SDS-PAGE. The separated proteins were subsequently blotted on a nitrocellulose membrane. The membrane was incubated with the polyclonal antibody against PRDX 2 (1:1000 dilution, Protein Tec Group, Chicago, IL, USA). The membrane was reacted with HRP-conjugated secondary antibody (1:1000 dilution, GE Healthcare Biosciences, Chicago, IL, USA). PRDX 2 was detected using an enhanced chemiluminesence system (GE Healthcare Biosciences, Chicago, IL, USA) and the LAS 3000 luminescent image analyzer (Fujifilm, Tokyo, Japan).

3 Results

We generated and compared the protein expression profiles between six good responders (Huvos grade 3/4) and six poor responders (Huvos grade 1) using 2-D DIGE. The clinicopathological parameters other than the responsiveness were not significantly different between these two groups. We detected 2250 protein spots that appeared in all the images of the Cy3-labeled internal control sample (Fig. 1C). The use of a large format 2-D system enabled to observe a relatively large number of protein spots. We identified 55 protein spots that are differentially expressed between the good and poor responders, performing a Kruskal–Wallis test with an applied Bonferroni adjusted *p*-value of <0.01. The localization of the 55 spots on the 2-D image is shown in Fig. 1C, whereas their intensity is shown in Fig. 2.

Mass spectrometric analysis resulted in the identification of 38 distinct gene products corresponding to the 55 protein spots (Fig. 2, Table 2, Supporting information Table 1).

We examined the correlation between the identified proteins and the prognostic information using several antibodies. After trials, we found that the use of a specific antibody against PRDX 2 confirmed the higher expression of PRDX 2 in the biopsy samples than from poor responders. In 2-D DIGE experiments, the PRDX 2 expression level inversely correlated with response to chemotherapy (Fig. 2), and the PRDX 2 levels measured by 2-D DIGE and Western blotting highly correlated (Fig. 3A). In an additional four cases, Western blotting showed that the expression of PRDX 2 was higher in the poor responders when compared with the good responders (Fig. 3B), thus confirming the results using the initial set of cases. Aberrant expression of PRDX 2 has been implicated in certain types of cancer such as human breast cancer [22]. PRDX 2 inhibited apoptosis, probably rendering tumor cells resistant

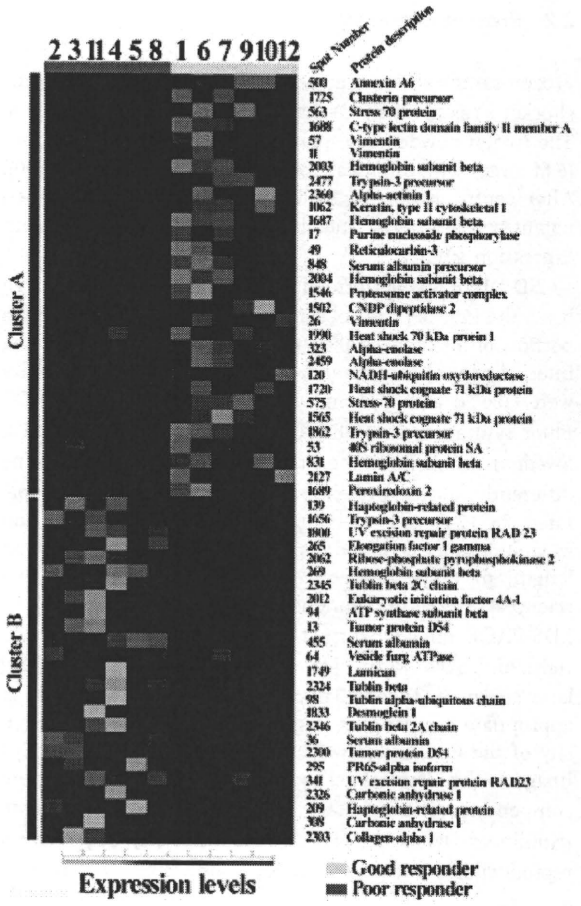

Figure 2. Hierarchical clustering of the 12 OS cases examined based on the intensity of the 55 protein spots detected. The cases are color-coded as yellow (good responder) or blue (poor responder) as indicated in the panel. The spot numbers and the protein names related proteins are shown on the right side.

to chemotherapeutic agents [23–25]. However, its association with OS has not been reported previously.

4 Discussion

High-throughput screening technologies such as the cDNA microarray technology have recently been employed to develop chemotherapy responsiveness biomarkers in OS. However, proteomic studies have not been performed using OS biopsy samples to date. Proteomic studies have unique advantages over other so-called -omics studies. The proteome is a functional translation of the genome, directly regulating cell phenotypes and is thus a rich source of biomarkers. With this notion, we have established a gel-based proteomics system for cancer research [21] and applied it to the OS proteomic study presented here in the first report using a proteomic approach to develop chemotherapy responsiveness biomarkers for OS.

Table 2. List of proteins identified by mass spectrometry

Spot no.[a)]	Prot_acc[b)]	Identified protein[b)]	Prot_pi[c)]	Prot_mass[c)]	Prot_score[d)]
500	ANXA6_HUMAN	Annexin A6	5.42	76168	628
1725	CLUS_HUMAN	Clusterin precursor	5.89	53031	109
563	GRP75_HUMAN	Stress-70 protein	5.87	73920	930
1688	CLC11_HUMAN	C-type lectin domain family 11 member A	5.06	36015	198
57	VIME_HUMAN	Vimentin	5.06	53676	373
11	VIME_HUMAN	Vimentin	5.06	53676	775
2003	HBB_HUMAN	Hemoglobin subunit β	6.75	16102	191
2477	TRY3_HUMAN	Trypsin-3 precursor	7.46	33276	114
1062	K2C1_HUMAN	Keratin, type II cytoskeletal 1	8.16	66149	247
2360	ACTN1_HUMAN	α-Actinin-1	5.25	103563	185
1687	HBB_HUMAN	Hemoglobin subunit β	6.75	16102	165
17	PNPH_HUMAN	Purine nucleoside phosphorylase	6.45	32325	187
49	RCN3_HUMAN	Reticulocalbin-3	4.74	37470	175
848	ALBU_HUMAN	Serum albumin precursor	5.92	71317	135
2004	HBB_HUMAN	Hemoglobin subunit β	6.75	16102	152
1546	PSME1_HUMAN	Proteasome activator complex subunit 1	5.78	28876	133
1502	CNDP2_HUMAN	CNDP dipeptidase 2	5.66	53187	435
26	VIME_HUMAN	Vimentin	5.06	53676	887
1990	HSP71_HUMAN	Heat shock 70 kDa protein 1	5.48	70294	590
323	ENOA_HUMAN	α-Enolase	7.01	47481	260
2459	ENOA_HUMAN	α-Enolase	7.01	47481	316
120	NDUS1_HUMAN	NADH-ubiquinone oxidoreductase	5.89	80443	94
1720	HSP7C_HUMAN	Heat shock cognate 71 kDa protein	5.37	71082	957
575	GRP75_HUMAN	Stress-70 protein	5.87	73920	372
1565	HSP7C_HUMAN	Heat shock cognate 71 kDa protein	5.37	71082	346
1862	TRY3_HUMAN	Trypsin-3 precursor	7.46	33276	97
53	RSSA_HUMAN	40S ribosomal protein SA	4.79	32947	462
831	HBB_HUMAN	Hemoglobin subunit β	6.75	16102	126
2127	LMNA_HUMAN	Lamin-A/C	6.57	74380	185
1689	PRDX2_HUMAN	PRDX 2	5.66	22049	377
139	HPTR_HUMAN	Haptoglobin-related protein	6.42	39496	128
1656	TRY3_HUMAN	Trypsin-3 precursor	7.46	33276	134
1800	RD23A_HUMAN	UV excision repair protein RAD23	4.56	39642	277
265	EF1G_HUMAN	Elongation factor 1-γ	6.25	50429	329
2062	PRPS2_HUMAN	Ribose-phosphate pyrophosphokinase II	6.15	35146	159
269	HBB_HUMAN	Hemoglobin subunit β	6.75	16102	270
2345	TBB2C_HUMAN	Tubulin β-2C chain	4.79	50255	446
2012	IF4A1_HUMAN	Eukaryotic initiation factor 4A-I	5.32	46353	914
94	ATPB_HUMAN	ATP synthase subunit β	5.26	56525	220
13	TPD54_HUMAN	Tumor protein D54	5.26	22281	346
455	ALBU_HUMAN	Serum albumin	5.92	71317	166
64	NSF_HUMAN	Vesicle-fusing ATPase	6.52	83021	355
1749	LUM_HUMAN	Lumican	6.16	38747	144
2324	TBB5_HUMAN	Tubulin β-chain	4.78	50095	815
98	TBAK_HUMAN	Tubulin α-ubiquitous chain	4.94	50804	142
1833	DSG1_HUMAN	Desmoglein-1	4.9	114670	334
2346	TBB2A_HUMAN	Tubulin β-2A chain	4.78	50274	372
36	ALBU_HUMAN	Serum albumin	5.92	71317	236
2300	TPD54_HUMAN	Tumor protein D54	5.26	22281	288
295	2AAA_HUMAN	PR65-α isoform	5	66065	263
341	RD23A_HUMAN	UV excision repair protein RAD23	4.56	39642	146
2326	CAH1_HUMAN	Carbonic anhydrase 1	6.59	28909	545
209	HPTR_HUMAN	Haptoglobin-related protein	6.42	39496	149
308	CAH1_HUMAN	Carbonic anhydrase 1	6.59	28909	516
2303	CO3A1_HUMAN	Collagen α-1	6.21	139733	164

a) Spot numbers refer to Figs. 1C and 2.
b) Proteins were derived from Swiss-Prot and the National Center for Biotechnology Information nonredundant databases.
c) Theoretical p*I* and molecular weight obtained from Swiss-Prot.
d) MASCOT score for the identified proteins based on the peptide ion score.